J Mater Sci: Mater Med (2008) 19:1953–1961
DOI 10.1007/s10856-007-3285-1

Formation of hydroxyapatite layer on bioactive Ti and Ti–6Al–4V by simple chemical technique

Achariya Rakngarm · Yukio Miyashita · Yoshiharu Mutoh

Received: 21 June 2007 / Accepted: 19 September 2007 / Published online: 18 October 2007

Abstract Bioactive coatings on cp-Ti and Ti–6Al–4V were prepared by a simple chemical technique. Specimens of cp-Ti and Ti–6Al–4V were initially immersed in a 5 M NaOH solution at 60 °C for 24 h which resulted in the formation of a porous network structure composed of $Na_2Ti_5O_{11}$ and TiO_2. The specimens were then immersed in a Ca-rich solution either at 60 °C or at 36.5 °C for 24 h. During this treatment Na^+ was released and Ti–OH groups were formed. Subsequently, TiO_2 dissociated from the Ti–OH group and combined with calcium ions to form calcium titanate ($CaTiO_3$), which was embedded in a titania gel layer during the immersion period. The specimens were then immersed in r-SBF at 36.5 °C for 1–30 days. After immersion in r-SBF for 3 days, HAp (hydroxyapatite) spheroids began to deposit on the substrates, and within a week the surfaces were covered. The HAp spheroids were 5 μm in size with a Ca/P ratio of 1.68 which was close to bone-like apatite (1.67). The average thicknesses of HAp layer after immersion in r-SBF for 3 days, 1 week, and 2 weeks were 3.8, 5.6, and 6.4 μm, respectively. A scratch test, used to evaluate the adhesive strength of the HAp layer, showed that the HAp layer was not scraped off until the applied load reached 26 N.

A. Rakngarm
Nagaoka University of Technology, 1603-1 Kamitomioka, Nagaoka-shi 940-2188, Japan

Y. Miyashita
Department of Mechanical Engineering, Nagaoka National College of Technology, 888 Nishikatakai, Nagaoka-shi 940-8532, Japan

Y. Mutoh (✉)
Department of System Safety, Nagaoka University of Technology, 1603-1 Kamitomioka, Nagaoka-shi 940-2188, Japan
e-mail: mutoh@mech.nagaokaut.ac.jp

1 Introduction

Titanium and its alloys have been used as artificial bone materials under biomechanical load bearing conditions, because they have excellent mechanical properties and non-toxic, i.e., when these materials are used as bone implants they are bioinert. Instead a fibrous tissue of variable thickness may form and encapsulate them, thereby isolating the implant material from the surrounding bone [1–3]. However, it has been reported that a bioactive Ti can be produced by alkali- and heat-treatments [2, 3, 11] and that resultant apatite coatings formed on the Ti surface in simulated body fluid (SBF) are similar to natural bone [3, 6, 11–13]. In order to develop bioactive surfaces with sufficient mechanical properties, several methods for coating the Ti surfaces with a bioactive ceramic, such as calcium phosphate, have been developed, including electrochemical deposition, plasma spraying, and chemical vapor deposition (CVD). Of these, the process that is most widely used commercially is plasma spraying [3].

However, the apatite/Ti interface and/or the coated apatite layer itself are sometimes fractured in vivo. Therefore implant materials which can survive in vivo without interface fracture between the coating layer and the substrate are required. It is therefore of interest that it has been reported that calcium ions from a surface oxide layer of calcium titanate ($CaTiO_3$) can enhance apatite precipitation and strengthen the interface between the coating layer and the substrate [4]. For the purpose of developing a $CaTiO_3$ layer on the substrate surface, it has been

thermodynamically shown that Ti pre-treated in NaOH solution can induce the formation of a $CaTiO_3$ layer [5]. In addition, some studies have found that the intermediate stage of the apatite precipitation on Ti and Ti alloys is the formation of $CaTiO_3$ from the titania-gel layer just after they have been immersed in the SBF solution after NaOH treatment [6, 7].

The apatite precipitation process takes some time for HAp formation and deposition to cover the entire surface if only an alkali or an acid treatment is used on the Ti implant materials, at least a month according to one in vitro study [12]. Since the growth of tissue around the implant materials would be faster than the apatite precipitation onto the implant materials, the tissue would isolate the implant material from the surrounding bone. Therefore a shorter time to develop HAp formation on the surface of implant materials is needed. Some studies tried to shorten the apatite formation time by using heat treatment with higher concentration of the simulated body fluid than the real body system, and thereby decreased the deposition time by up to 10 days [8, 9]. Calcium titanate ($CaTiO_3$) is one of the possible materials to shorten the HAp formation time and accelerate growth of tissue into the implant materials. However, no research work related to the behavior and strength of HAp formation from $CaTiO_3$ has been reported.

Therefore, in the present study the attempt was made to strengthen the HAp layer and the interface between the HAp layer and the Ti substrate by creating a calcium-ion-containing layer and/or a $CaTiO_3$ layer on substrates of Ti and its alloys. Surface treatments of the substrate before coating by several chemical reactions were applied to achieve higher bonding strength between the HAp layer and the substrate. The adhesive strength between the coating layer and the substrate was investigated by using a scratch test machine.

2 Experimental procedures

2.1 Alkali treatment by NaOH

Flat sheets, 3 mm thick and 50 mm × 10 mm, of commercially pure titanium (cp-Ti) and of Ti–6Al–4V were used in this study as substrate materials. The rectangular substrates were ultrasonically cleaned in distilled water, acetone, and ethanol for 20 min/each, after which the substrate plates were ultrasonically cleaned again in distilled water for another 10 min. Subsequently, the cleaned substrate plates were immersed in 5 and 10 M NaOH at 60 °C for 24 h. After the 24 h incubation period, the substrates were gently washed with distilled water and dried in air.

2.2 Ca-rich solution

After the treatment with NaOH, the cp-Ti and Ti–6Al–4V substrates were immersed in a calcium-rich (saturated $Ca(OH)_2$) solution at temperatures and for times shown in Fig. 1. After this the substrates were rinsed well with distilled water and dried in air. At least 10 specimens were used for each test condition in order to confirm the reproducibility of the results.

2.3 Apatite precipitation in r-SBF

Finally, the treated cp-Ti and Ti–6Al–4V substrates were soaked in revised-simulated body fluid (r-SBF), details of which have been described by Oyane et al. [10]. The r-SBF was prepared by dissolving reagent grade NaCl, $NaHCO_3$, Na_2CO_3, KCl, $K_2HPO_4{\cdot}3H_2O$, $MgCl_2{\cdot}6H_2O$, $CaCl_2$, and Na_2SO_4 into de-ionized water and buffering at pH 7.40 at 36.5 °C with HEPES (2-(4-(2-hydroxyethyl)-1-piperazinyl) ethanesulfonic acid) and 1.0 M NaOH aqueous solution. The r-SBF is a solution with ion concentrations nearly equal to those of human blood plasma, as shown in Table 1. The treated substrates were immersed in r-SBF at 36.5 °C for 1 day up to 30 days. The r-SBF was refreshed every 2 days in order to preserve its ion concentration.

2.4 Characterization of the coating

The heat treatment was conducted to confirm the existing phases after immersed in NaOH solution, Ca-rich solution, where the treated plates were heated up to 600 °C at a heating rate of 5 °C/min in an electric furnace, kept at 600 °C for an hour and then allowed to cool in the furnace.

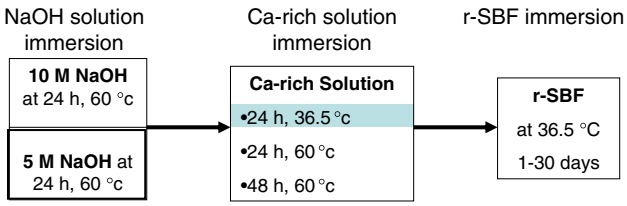

Fig. 1 Schematic of the surface modifications

Table 1 Ions concentration of the solution used for apatite precipitation

	Na^+	K^+	Ca^{2+}	Mg^{2+}	HCO_3^-	Cl^-	HPO_4^-	SO_4^{2-}
Blood plasma	142.0	5.0	2.5	1.5	27.0	103.0	1.0	0.5
r-SBF	142.0	5.0	2.5	1.5	27.0	103.0	1.0	0.5

After the heat treatment, the following observation and characterization were carried out. The morphology of specimen surface was observed by a scanning electron microscope (SEM/EDS, JEOL JSM 6360 A) operating at 20 kV. The surface chemical analysis was carried out by an energy dispersive X-ray spectroscopy (EDS), which was coupled to SEM. The crystalline phases of the coating were identified by X-ray diffraction (XRD, Philips XRD 6100) analysis. XRD using grazing incident of 2° was performed on the cp-Ti and Ti–6Al–4V surface after each step of the coating procedure. XRD was carried out using Cu-K_α radiation operating at 40 kV and 30 mA. The coating layer thickness was evaluated by cross-sectional observation. After each step in the overall process specimens of the cp-Ti specimens were mounted in epoxy resin and polished to the mirror-surface condition to determine the average coating layer thickness. The thickness was defined as the average of five coating-layer measurements.

2.5 Scratch tests for evaluating the adhesive strength

Scratch test was carried out to evaluate the adhesive strength between the coating layer and the substrate after immersion in r-SBF. A commercial scratch test machine of normal load increasing type was used and the scratch tests were carried out in conformity with JSME standard S 010 [14]. A diamond Vickers indenter with 200 μm tip radius was moved across the specimen surface under a pre-load of 0.9 N at a speed of 10 mm/min with an increasing normal load rate of 100 N/min. The maximum applied load was 100 N. The total distance of each scratch trace was 10 mm. Three scratch tests were conducted for each specimen. After the scratch test, the scratch tracks were observed by an optical microscope in order to determine the point at which local delamination occurred in the coating layer. The critical loading was defined as the average of the three values at the point where delamination occurred in each scratch trace.

3 Results and discussion

3.1 Alkali treatment by NAOH and Ca-rich solution

The surfaces of both cp-Ti and Ti–6Al–4V substrates after immersion in 5 and 10 M NaOH at 60 °C exhibited a thin, porous network structure, as shown in Fig. 2. As can be seen from Fig. 2a and b, cracks were found on the specimen immersed in 10 M NaOH. However they were not found on specimens immersed in 5 M NaOH, as seen from Fig. 2c and d. The pore size of the porous network structure, about 100–300 nm, did not depend upon the concentration of the NaOH solution.

Figure 3 shows the results of XRD analysis of (a) the cp-Ti surface after immersion in 5 M NaOH , (b) the surface of Ti–6Al–4V after immersion in 5 M NAOH, after immersion in 5 M NaOH, (c) the surface of cp-Ti after immersion in 5 M NaOH followed by heat treatment at 600 °C and (d) the surface of Ti–6Al–4V after immersion in 5 M NaOH and heat treatment at 600 °C. Sodium titanate ($Na_2Ti_5O_{11}$) and titanium oxide or rutile (TiO_2) peaks appeared on all XRD patterns, but were more prominent after heat treatment. The EDS analysis of this porous

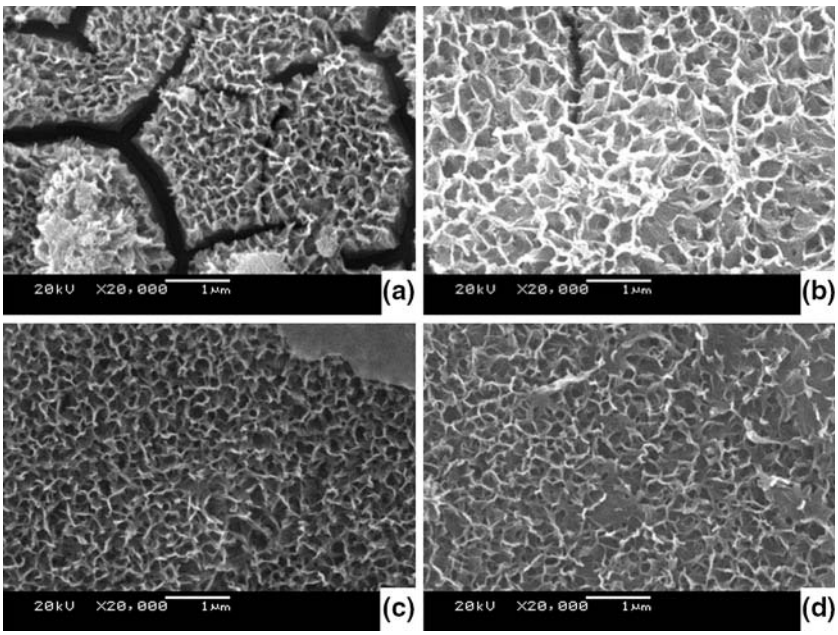

Fig. 2 Surface morphology for (**a**) cp-Ti and (**b**) Ti–6Al–4V substrates after treatment in 10 M-NaOH at 60 °C for 24 h, and (**c**) cp-Ti and (**d**) Ti–6Al–4V substrates after treatment in 5 M-NaOH at 60 °C for 24 h

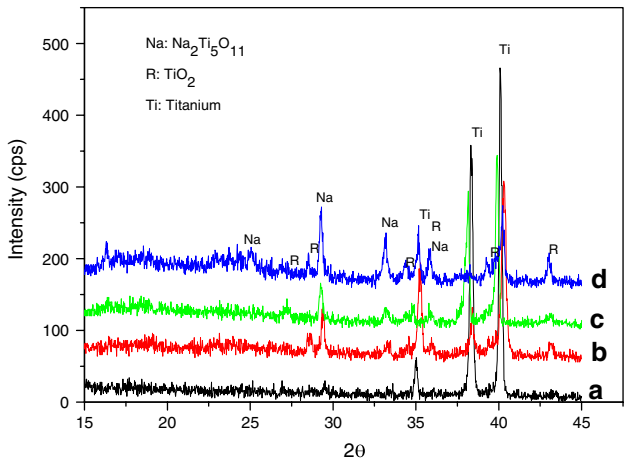

Fig. 3 Crystalline phases existing on the surfaces of (**a**) cp-Ti and (**b**) Ti–6Al–4V substrates after immersed in 5 M NaOH, and (**c**) cp-Ti and (**d**) Ti–6Al–4V substrates after heat treated at 600 °C

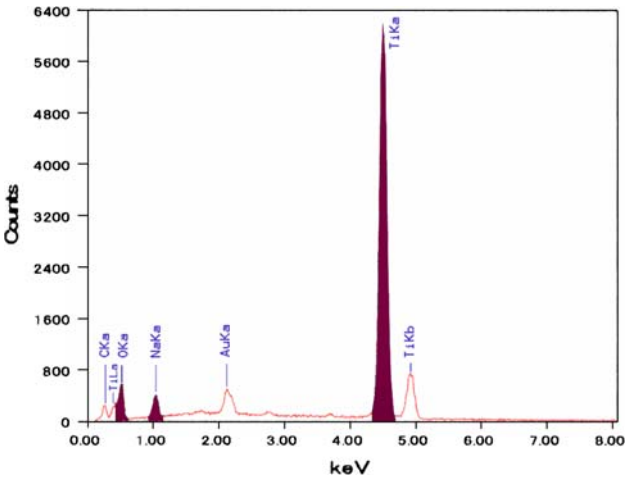

Fig. 4 EDS analysis of the porous network structure after treated with 5M-NaOH

network indicated the presence of Na, Ti, and O-atoms (Fig. 4), in agreement with the result of the XRD analysis. The broadened peaks found in specimens without heat treatment indicated the existence of an amorphous hydrogel phase consisting of $Na_2Ti_5O_{11}$ and TiO_2. During heat-treatment at 600 °C, crystallization of $Na_2Ti_5O_{11}$ and TiO_2 phases occurred. It is proposed that during drying of the NaOH treated specimens, the shrinkage of the hydrogel phases caused cracks to appear on the surface of the 10 M NaOH treated specimens.

According to Refs. [4, 8–13], during immersion in NaOH solution, an amorphous $Na_2Ti_5O_{11}$ and TiO_2 hydrogel layer dissolves into the alkaline solution because of the presence of a corrosive hydroxyl group within the hydrogel layer. Gil et al. [13] described the process of $Na_2Ti_5O_{11}$ and TiO_2 formation during alkali treatment as follows:

$$TiO_2 + OH^- \rightarrow HTiO_3^- \quad (1)$$

This reaction proceeds simultaneously with the following hydration reaction of the Ti-based substrate,

$$Ti + 3OH^- \rightarrow Ti(OH)_3^+ + 4e^- \quad (2)$$

$$Ti(OH)_3^+ + e^- \rightarrow TiO_2 + H_2O + 0.5H_2(g) \quad (3)$$

$$Ti(OH)_3^+ + OH^- \leftrightarrow Ti(OH)_4 \quad (4)$$

As the hydroxyl groups are produced they will attack TiO_2 and the hydrated TiO_2 will generate negative charges on the surface of the substrates as follows:

$$TiO_2 \cdot nH_2O + OH^- \leftrightarrow HTiO_3^- nH_2O \quad (5)$$

During the alkali treatment, a low solute concentration of NaOH develops near the solid surface [12]. Since the thickness of the deposited region is controlled by the reaction rate, the porous network structure of $Na_2Ti_5O_{11}$ gel layer obtained from 10 M NaOH alkali treatment is thicker than the gel layer obtained from 5 M NaOH alkali treatment. Since the gel layer obtained from 5 M NaOH alkali treatment was thinner, shallower in pore shape, and of lower water content as compared to the gel layer from 10 M NaOH alkali treatment, shrinkage cracks were not developed after drying. The negatively charged species indicated in Eq. 5 easily combine with alkali and/or other positive ions in the aqueous solution, resulting in the formation of a $Na_2Ti_5O_{11}$ layer. During the heat treatment process, the hydrogel is dehydrated and densified, leading to a well-crystallized $Na_2Ti_5O_{15}$ layer.

Substrates of cp-Ti and Ti–6Al–6V after the 5 M-NaOH treatment were immersed in calcium-rich (saturated $Ca(OH)_2$) solution at 60 °C for 24 and 48 h, or at 36.5 °C for 24 h to provide Ca-rich layer. The pH value of this saturated $Ca(OH)_2$ aqueous solution was 13.23. In this pH region the porous network structure was not destroyed. Moreover, Ca-ion precipitation is expected to occur from the basic Ca-rich solution.

The surface layer after immersion in the Ca-rich solution at 36.5 °C for 24 h consisted of a porous hydrogel network structure containing many of small, spongy islands, as shown in Fig. 5. The surfaces after immersed in Ca-rich solution at 60 °C for 24 and 48 h showed a porous network and the presence of calcium and carbon, which suggests the presence of calcium carbonate ($CaCO_3$) on the surface. However, the EDS analysis of the particles on the specimen treated with Ca-rich solution at 36.5 °C for 24 h showed the presence of uniformly distributed calcium ions. It is supposed that these network structures were in an ionic state on the specimen surface. After heat treatment at

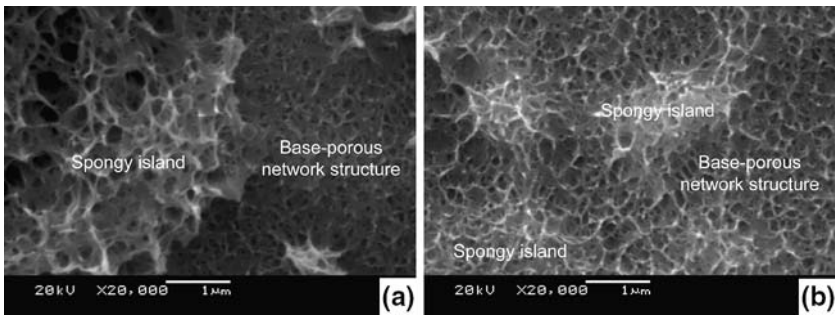

Fig. 5 Surface morphology of 5 M-NaOH treated surfaces after immersion in Ca-rich solution at 36.5 °C for 24 h for (**a**) cp-Ti and (**b**) Ti–6Al–4V substrates

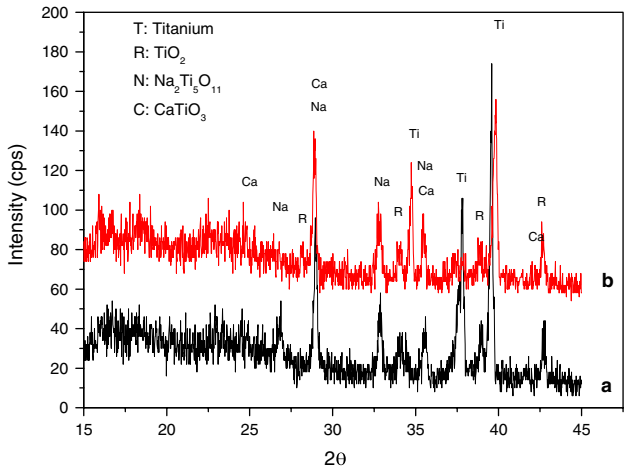

Fig. 6 Crystalline phases existing on the specimen surfaces after immersion in Ca-rich solution and heat treatment at 600 °C for (**a**) cp-Ti and (**b**) Ti–6Al–4V substrates

600 °C, a small amount of the crystalline phase $CaTiO_3$ was found, as can be seen in Fig. 6.

During the Ca-rich solution treatment, the sodium titanate hydrogel was partially dissolved into the Ca-rich solution. Since the Na^+ ion dissolved into the solution, the Ti–OH group formed on the substrate surface immediately after Na^+ was released. The Ti–OH group, immediately after their formation, incorporated the calcium ions in the solution to form $CaTiO_3$. In addition, TiO_2 existed in the gel layer as an amphoteric oxide which inhibited the formation of hydrated Ti–OH groups. This produced a large number of negative charges on the surface as in reactions (1)–(4). $CaTiO_3$ may deposit in accordance with the following reactions:

$$Ti(OH)_3^+ + OH^- \leftrightarrow Ti(OH)_4 \quad (6)$$

$$Ca(OH)_2 \rightarrow Ca^{2+} + 2(OH)^- \quad (7)$$

$$Ca^{2+} + Ti(OH)_4 \rightarrow CaTiO_3 + 2H^+ + H_2O \quad (8)$$

Takadama et al. [6] explained the $CaTiO_3$ formation as follows. The starting stage of CaTiO3 formation is proposed to be an electrostatic formation of negative charges of titania (TiO_2) dissociated from the Ti–OH group with the positive charge calcium ions in the Ca-rich solution. Then the migration of Ca^{2+} from the solution to the Ti-substrate with embedment in the titania gel layer was occurred continuously during the immersion period. This thin and uniformly bonded $CaTiO_3$ layer on the surface oxide is expected to enhance apatite precipitation, and is also expected to achieve higher bonding strength.

3.2 Deposition of HAp by r-SBF solution

The coating layer on the cp-Ti and Ti–6Al–4V substrates during immersion in the r-SBF solution promoted the deposition of calcium phosphate within a few days of immersion. Figure 7 shows the SEM micrographs of the surface morphology of the specimens after different periods of soaking in r-SBF. The images clearly show that calcium phosphate started to deposit on the substrate within a day. Isolated spheroidical islands of diameter less than 5 μm were clearly observed after immersion in r-SBF for 3 days, as seen from Fig. 7b and g, and the entire surface was covered within a week as seen in Fig. 7c and h. The image of as-deposited primary particles clearly showed tiny round particles of approximate diameter of 10–20 nm, as shown in Fig. 8.

Table 2 shows Ca/P ratio after immersed in r-SBF for various periods. The EDS analysis of the spheroids after immersion for 3 days in r-SBF showed the presence of calcium and phosphate with a Ca/P molar ratio greater than 2. Since the Ca/P ratio for calcium phosphate is known to be less than 2, Ca-ions may have been embedded in the surfaces. The Ca/P ratio of the spheroids after immersion in r-SBF for a week was 1.65–1.68, which was close to that of bone-like apatite, 1.67. The attained value of the Ca/P ratio was almost constant even after longer immersion in r-SBF, in agreement with the results of XRD analysis shown in Fig. 9. The diffraction patterns showed broadened hydroxyapatite peaks at 2θ = 30–33°, as seen from Fig. 9. Although the peaks of $CaTiO_3$, $Na_2Ti_5O_{11}$, and TiO_2 remained after various of immersion periods, the peak intensities of $CaTiO_3$, $Na_2Ti_5O_{11}$, and TiO_2 decreased with

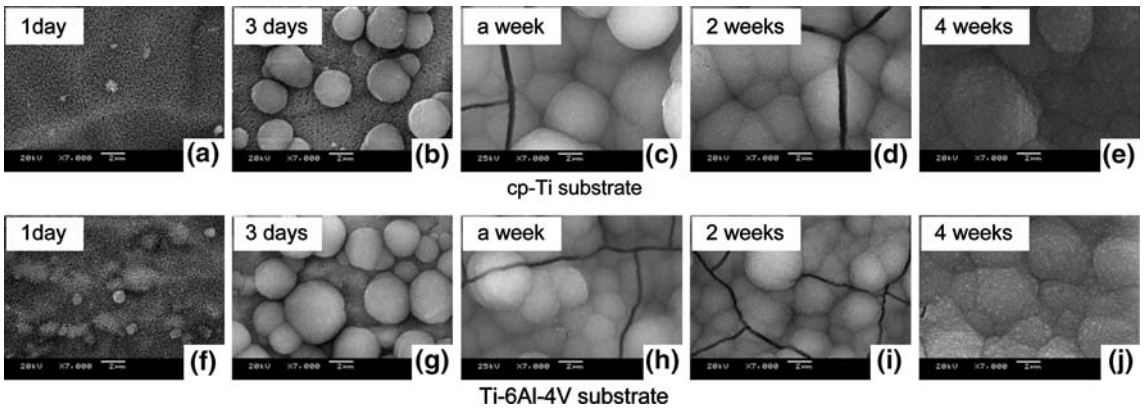

Fig. 7 Surface morphology of specimens immersed in the r-SBF for various periods

Fig. 8 As-deposited HAp primary particles as observed in SEM

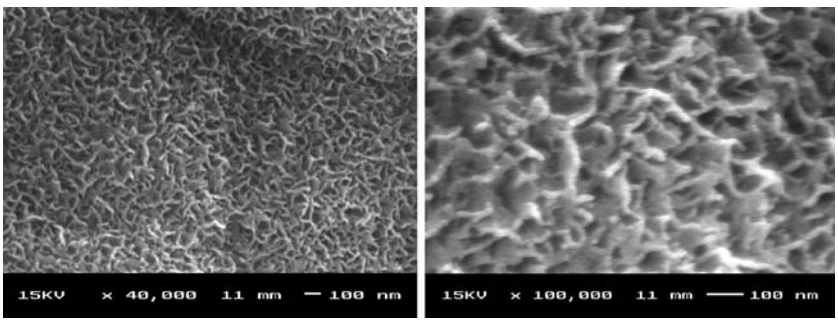

Table 2 Ca/P ratio after immersion in r-SBF for various periods

		Ca-ion (mole)	P-ion (mole)	Ca/P (mole ratio)
cp-Ti	1 day	0.019	N/A	N/A
	3 days	0.388	0.186	2.08
	1 week	0.703	0.411	1.71
	2 weeks	1.039	0.618	1.68
Ti–6Al–4V	1 day	0.090	0.005	17.49
	3 days	0.298	0.171	1.75
	1 week	0.687	0.416	1.65
	2 weeks	0.789	0.462	1.71

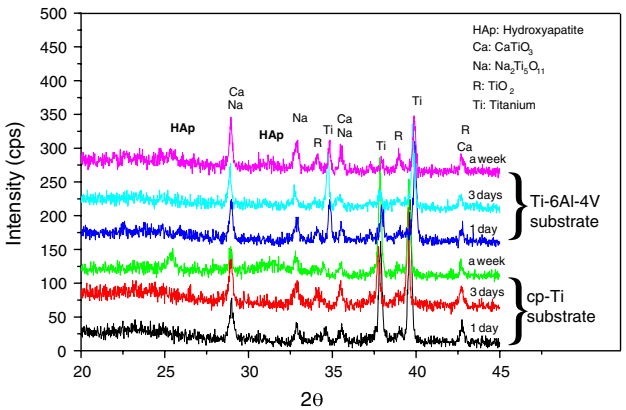

Fig. 9 Crystalline phases existing on the specimen at different immersion periods for cp-Ti and Ti–6Al–4V substrates, respectively

increase of the HAp peak intensity, and HAp dominated after prolong immersion times.

According to Coreno et al. [15], calcium ions are leached from $CaTiO_3$ at room temperature as a function of pH. Since the pH of r-SBF was maintained at 7.4 at a constant temperature of 36.5 °C, the CaTiO3 reacted with water as follows:

$$CaTiO_3 + H_2O \rightarrow Ca^{2+} + TiO_2 + 2OH^- \quad (9)$$

When exposed to r-SBF, an increase of the OH^- group at the liquid/solid interface will increase the pH value of the solution. The hydrogel layer in r-SBF might exhibit a positive charge due to the presence of Ca^+. The positively charged Ca^{2+} will act as a nucleation site for HAp by reacting with the negatively charged PO_4^{3-} to form a Ca-P enriched surface layer according to the following reaction:

$$10Ca^{2+} + 6PO_4^{3-} + 2OH^- \rightarrow Ca_{10}(PO_4)_6(OH)_2 \quad (10)$$

In the present experiments, HAp began to deposit within 24 h after immersion in r-SBF and completely covered the entire surface of Ti substrate within a week, which is much faster than in the cases of only alkali treatment Ti (a month [12]), or acid treatment (10 days [1]).

3.3 Adhesive strength

Figure 10 shows the average critical loads (L_c: the load at which local delamination of coating was observed on the scratch track [14]) of the coating after different immersion periods in r-SBF. As can be seen from the figure, the HAp layer of the specimens immersed in r-SBF for 1 week up to 4 weeks when the HAp layer completely covered on the surface, sustained at least a normal load of 26 N. The critical load decreased with decreasing the immersion time. The HAp layers after immersion in r-SBF for various times are shown in Fig. 11. As seen from the figure, the average thickness of HAp layer after immersion in r-SBF for 1 day, 3 days, a week, 2 weeks, and 4 weeks were 2.2, 3.8, 5.6, 6.4, and 10.2 μm, respectively. From Fig. 10, it seems that the prolonged soaking time and the thickness of the specimen did not have much effect on the adhesive strength. Figure 12 shows optical micrographs of the scratch tracks at the critical load.

These adhesive strength results were compared with the strength of other coatings developed by other techniques, i.e., PVD-TiC (PVD: Physical Vapor Deposition), CVD-TiC (CVD: Chemical Vapor Deposition) and PVD-TiN coating [16]. The same JSME standard procedure was used in both the present study and in [16] . In [16, thicknesses of PVD-TiC, CVD-TiC, and PVD-TiN were 4.6, 4.6, and 3.8 μm, respectively. The critical loads for PVD-TiC and CVD-TiC were 25 N and 22 N, respectively, which were almost in the same range as the present critical load, although, the critical load for PVD-TiN was higher, 70 N. The average adhesive strengths of the coating on cp-Ti were 23 N for 3 days immersion in r-SBF and 26 N for 1-week immersion in r-SBF. The thicknesses of HAp coating layer of 3 days and a week immersed in r-SBF were 3.8 and 5.6 μm, respectively. It is noted that the adhesive strengths of the present HAp coating were at same level as for TiC coatings, which are used for wear resistant coatings for cutting tools. The main reason for the high adhesive strength value of the present HAp coating is attributed to the formation of a $CaTiO_3$/TiO_2 interlayer between the substrate and the HAp top layer.

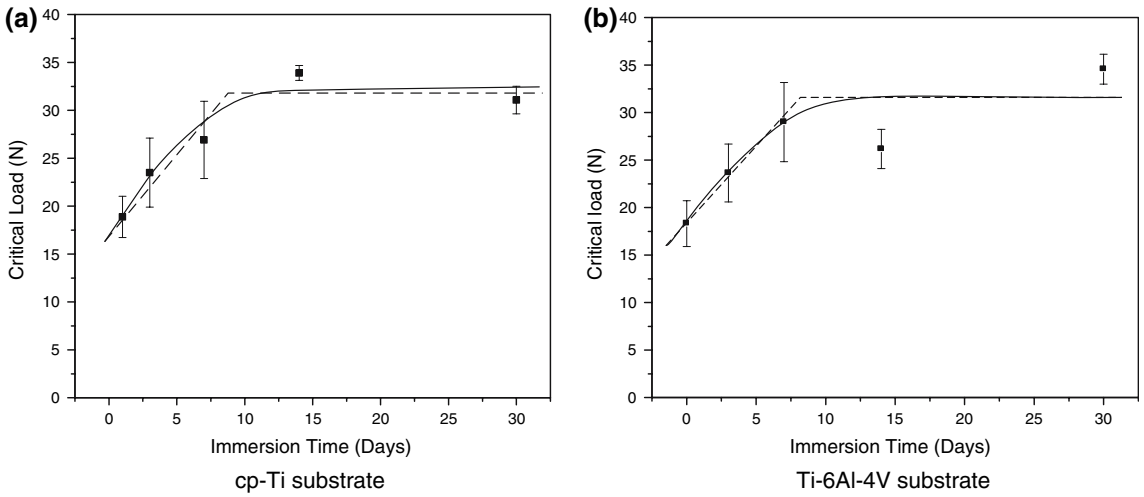

Fig. 10 Relationship between the average critical load and immersion time in r-SBF for (**a**) cp-Ti and (**b**) Ti–6Al–4V substrates

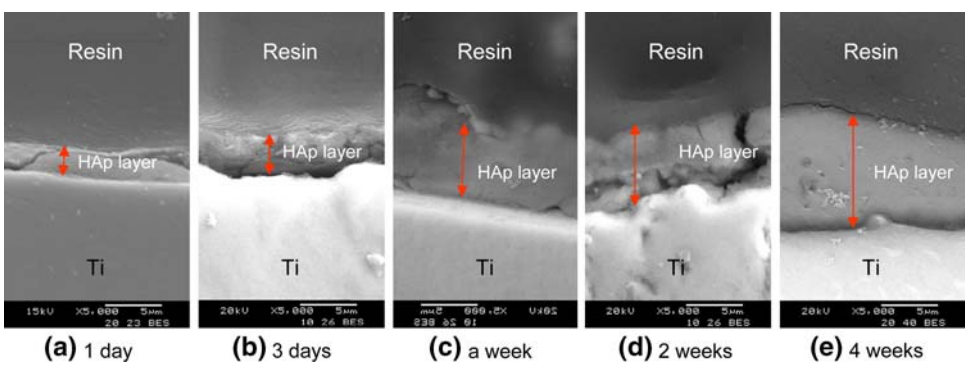

Fig. 11 Cross-sections showing the development of HAp layers after various times in r-SBF solution

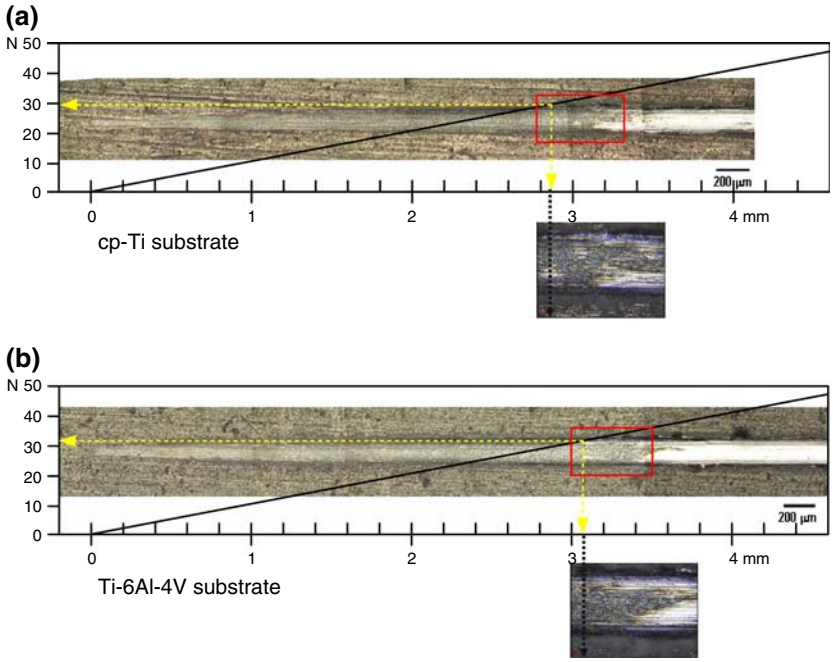

Fig. 12 Scratch track observations at the critical load after immersion in r-SBF for a week; (**a**) cp-Ti substrate and (**b**) Ti–6Al–4V substrate. Delaminated region is the white appearing region at right of scratch

4 Conclusions

A new process for forming a HAp layer of high adhesive strength on a TiH-based substrate was successfully developed. The main findings and conclusions obtained are summarized as follows:

1. (a) After immersion of cp-Ti and Ti–6Al–4V substrates in 5 M NaOH at 60 °C, a porous network structure with inter-connecting pore consisting of $Na_2Ti_5O_{11}$ and TiO_2 developed on the surfaces of the substrates. The average pore size was 100–300 nm.
   (b) After subsequent immersion in a Ca-rich solution, a Ca-ion distribution and $CaTiO_3$ co-existing with TiO_2 formed on the surface.
   (c) After further immersion in r-SBF solution for 3 days, isolated HAp islands of an average size of 5 µm were observed, and the entire specimen surface was covered within a week. The Ca/P ratio of HAp spheroids was 1.68, which was close to the value for bone-like apatite.
2. Even for immersion periods in r-SBF of less than 1 week, HAp layer was formed as the result of the embedded Ca-ion and $CaTiO_3$ on the surface promoting HAp precipitation and thereby accelerating the deposition rate of HAp.
3. From the results of scratch tests, it is found that the HAp layer did not delaminate below a normal load of 26 N, which is about equal to the critical load for PVD-TiC and for CVD-TiC coating layers. A main reason for the high adhesive strength of the present HAp coating is existence of $CaTiO_3$ which contributes to the adhesive strength through the formation of a $CaTiO_3/TiO_2$ interlayer between the substrate and the HAp top layer. Ca-ions co-existing between the $CaTiO_3/TiO_2$ and HAp ($Ca_{10}(PO_4)_6(OH)_2$) layers may also contribute the adhesive strength.

Acknowledgement The authors wish to thank Prof. A. J. McEvily, University of Connecticut, for his help to improve the manuscript.

References

1. L. JONASOVA, F. A. MULLER, A. HELEBRANT, J. STRNAD and P. GREIL, *Biomaterials* **25** (2004) 1187
2. S. NISHIGUCHI, T. NAKAMURA, M. KOBAYASHI, F. MIYAJI and T. KOKUBO, *Biomaterials* **20** (1999) 491
3. L. L. HENCH, *J. Am. Ceram. Soc.* **81** (1998) 1705
4. K. HAMADA, M. KON, T. HANAWA, K. YOKOYAMA, Y. MIYAMOTO and K. ASAOKA, *Biomaterials* **23** (2002) 2265
5. M. C. De ANDRADE, M. R. T. FILGUEIRAS, T. OGASAWARA, *J. Biomed. Mater. Res.* **46** (1999) 441
6. H. TAKADAMA, H. M. KIM, T. KOKUBO and T. NAKAMURA, *Sci. Technol. Adv. Mater.* **2**(2) (2001) 389
7. H. TAKADAMA, H.M. KIM, T. KOKUBO and T. NAKAMURA, *J. Biomed. Mater. Res.* **57** (2001) 441
8. A. BIGI, E. BOANINI, B. BRACCI, A. FACCHINI, S. PANZAVOLTA, F. SEGATTI and L. STURBA, *Biomaterials* **26** (2005) 4085
9. C. M. DE ASSIS, L. C. DE OLIVEIRA VERCIK, M. L. SANTOS, M. V. LIA FOOK and A. C. GUASTALDI, *Mat. Res.* **8**(2) (2005) 207
10. A. OYANE, H. M. KIM, T. FURUYA, T. KOKUBO, T. MIYAZAKI and T. NAKAMURA, *J. Biomed. Mater. Res. A.* **65** (2003) 188
11. J. H. LIN, C. H. CHANG, Y. S. CHEN and G. T. LIN, *Surf. Coat. Tech.* **200** (2006) 3665

12. F. LIANG, L. ZHOU and K. WANG, *Surf. Coat. Tech.* **165** (2003) 133
13. F. J. GIL, A. PADROS, J. M. MANERO, C. APARICIO, M. NILSSON and J. A. PLANELL, *Mat. Sci. & Eng. C.* **22** (2002) 53
14. JSME Standard JSME S 010, in "Standard method for evaluating the defects in the coatings made by Dry processings" (The Japan Society of Mechanical Engineers, 1996) p. 6
15. J. CORENO and O. CORENO, *J. Biomed. Mat. Res. A.* **75** (2005) 478
16. Y. MIYASHITA, Y. SASAKI, T. KUROISHI, T. WATANABE, J. Q. XU, Y. MUTOH and M. YASUOKA, *JSME Int. J.* **46**(3) (2003) 335